Talanta 134 (2015) 425–434

Contents lists available at ScienceDirect

Talanta

journal homepage: www.elsevier.com/locate/talanta

One-step synthesis of sub-2 μm vinyl functionalized silica sphere as stationary phase for liquid chromatography

Yuming Xie, Xiaoqiong Zhang, Qiang Han, Wei Wan, Mingyu Ding *

Beijing Key Laboratory of Microanalytical Methods and Instrumentation, Department of Chemistry, Tsinghua University, Beijing 100084, China

ARTICLE INFO

Article history:
Received 23 September 2014
Received in revised form
19 November 2014
Accepted 20 November 2014
Available online 29 November 2014

Keywords:
Sub-2 μm vinyl-functionalized silica sphere
Cycle-model
Thiol-ene reaction
High performance liquid chromatography
Stationary phase

ABSTRACT

Vinyl-functionalized silica spheres (VFSS) were synthesized through the one-step method. The effects of reactant ratio, temperature, reaction time and ammonium hydroxide dripping speed were investigated. The diameter of the spheres reached sub-2 μm magnitude by controlling the reaction conditions, which is suitable for high performance liquid chromatography (HPLC) packing material. The vinyl groups in the silica spheres were further successfully modified by octadecyl (C_{18}) groups through a "thiol-ene" click reaction. Raw VFSS and C_{18}modified VFSS (C-VFSS) were used as HPLC stationary phases to separate benzene homologs (benzene, toluene, and meta-xylene) and nonpolar compounds with different ring contents (benzene, phenantherene and fluoranthene). Both VFSS and C-VFSS exhibited hydrophobic retention behavior. Additionally, vinyl groups in the silica spheres may offer a π–π electron–donor–acceptor (EDA) retention mechanism for chromatographic separation.

1. Introduction

HPLC is one of the most widely used analytical methods. A separation column is a key component in an HPLC instrument. Several kinds of materials have been successfully used as HPLC stationary phase, such as porous silica, ceramic materials, and metal-organic frameworks, among others [1–4]. However, silica spheres are the most common packing materials used in HPLC because of the high mechanical strength, uniform morphology and low cost. Silica spheres are generally synthesized using the Stöber method [5]. However, the synthesized silica spheres are decorated by hydroxyl group, which does not enable use of several modifying methods because of insufficient chemical activity. Replacing the hydroxyl group with active functional groups that can adapt to more modifications is an effective solution to this problem [2,6–8].

Among the modifying techniques available, "click chemistry" is one of the most effective methods. Click chemistry is a concept described by Sharpless in 2001 [9], which represents a series of chemical reactions that exhibit advantages including simple reaction condition, rapid reaction speed, good selectivity, high conversion, and environmentally-friendly reaction. "Thiol-ene" reaction, which was first reported by Posner in 1905 [10], satisfies all of the requirements specified above. The free-radical reaction may be used in several fields, such as polymer functionalization, surface modification, drug carrier synthesis, and imprint lithography [11–14]. Some studies used "thiol-ene" reaction to modify the HPLC packing material. Liang synthesized various chromatographic packing materials using "thiol-ene" reaction to separate saccharides and peptides [15–17]. Wang produced a monolith column through "thiol-ene" reaction to separate derivatives and organic acids [18]. Peng fabricated a novel carboxyl stationary phase by "thiol-ene" reaction to be used in hydrophilic interaction chromatography [19]. Furthermore, Chen produced a hybrid monolith capillary column through "click" reaction to separate nucleosides [20]. Chromatographic performances of their columns indicated that "thiol-ene" reaction is a good method to modify packing materials. However, this method is not suitable for directly synthesized silica spheres because these materials do not contain a superficial "thiol" or "ene". To the best of our knowledge, all silica stationary phases modified through "thiol-ene" reaction, except for monolith, require a time-consuming post-grafting step. Directly synthesizing functionalized silica packing materials is necessary to overcome this disadvantage. "Ene" is a more versatile functional group compared with "thiol" because "ene" may also be utilized in traditionally polymerizing vinyl-functionalized monomers [21–23]. Thus, synthesizing vinyl-functionalized silica spheres (VFSS) is a reasonable strategy.

Abbreviations: VFSS, Vinyl-functionalized silica spheres; $NH_3 \cdot H_2O$, Ammonium hydroxide; C_{18}, Octadecyl; HPLC, High performance liquid chromatography; C-VFSS, C_{18} modified vinly-functionalized silica spheres; EDA, Electron-donor-acceptor; VTES, Vinyltriethoxysilane; TEOS, Teraethyl orthosilicate; AIBN, 2,2-Azobisisobutyronitrile; SEM, Scanning electron microscopy; FT-IR, Fourier transform infrared spectroscopy analysis

* Correspondence to: Department of Chemistry, Tsinghua University, Beijing 100084, PR China. Tel.: +86 10 62797087; fax: +86 10 62781106.
E-mail address: dingmy@mail.tsinghua.edu.cn (M. Ding).

http://dx.doi.org/10.1016/j.talanta.2014.11.044
0039-9140/

Some researchers have directly fabricated VFSS successfully. Pu synthesized VFSS using polystyrene as a template and vinyltriethoxysilane (VTES) as a precursor. Spheres fabricated in the study vary in diameter from 100 nm to 150 nm [24]. Yasunari prepared VFSS through a one-pot method that used tetraethyl orthosilicate (TEOS) and VTES as precursors. A template is not necessary in this method, and diameters of spheres produced ranged from 50 nm to 130 nm [25]. Deng proposed a simple method to synthesize VFSS [26–28]; in this method, only three reactants (H_2O, VTES, and $NH_3 \cdot H_2O$) are used. Particle size is adjusted from 420 nm to 650 nm by varying the reaction conditions used. Spheres produced are ultra-uniform; however, size of VFSS produced did not satisfy the requirements for HPLC application. To our knowledge, sub-2 μm is the minimum size required for HPLC packing materials. Spheres with smaller size demonstrated difficulty in packing, and column back pressure would beyond the limit of most instruments [29–31].

In this work, the VFSS was synthesized using a one-step method, which could effectively enlarge the diameter of the VFSS. By controlling the reaction conditions, the final diameter of the VFSS reached 1.82 μm, which meets the size requirement of HPLC packing materials. Moreover, the VFSS was successfully modified through a "thiolene" click reaction. Both the VFSS and C_{18} modified-VFSS (C-VFSS) were used as an HPLC stationary phase to effectively separate benzene homologs (benzene, toluene, and meta-xylene) and nonpolar compounds with different ring contents (benzene, phenantherene and fluoranthene). The chromatographic performances of the columns show that the materials exhibit hydrophobic retention behavior. Additionally, the chromatographic retention behaviors of p-nitroaniline, aniline, p-chloroaniline on VFSS column prove that vinyl groups in the silica spheres may offer a π–π electron–donor–acceptor (EDA) retention mechanism for chromatographic separation.

2. Experimental

2.1. Chemicals

The VTES, TEOS, benzene, toluene and 2,2-azobisisobutyronitrile(AIBN) were purchased from Beijing Chemical Co., Ltd. Meta-xylene was acquired from Beijing Jinlong Chemical Co., Ltd., and $NH_3 \cdot H_2O$ (25% to 28%) was obtained from Xilong Chemical Co. Ltd. 1-octadecanethiol was purchased from Alfa Aesar. Meanwile, aniline, p-chloroaniline, and p-nitroaniline were procured from Sinopharm Chemical Reagent Co., Ltd. Fluoranthene and phenanthrene were obtained from TCI Chemical Reagent Co., Ltd., and acetonitrile was purchased from Fisher Scientific. All of the chemicals were used directly without further purification.

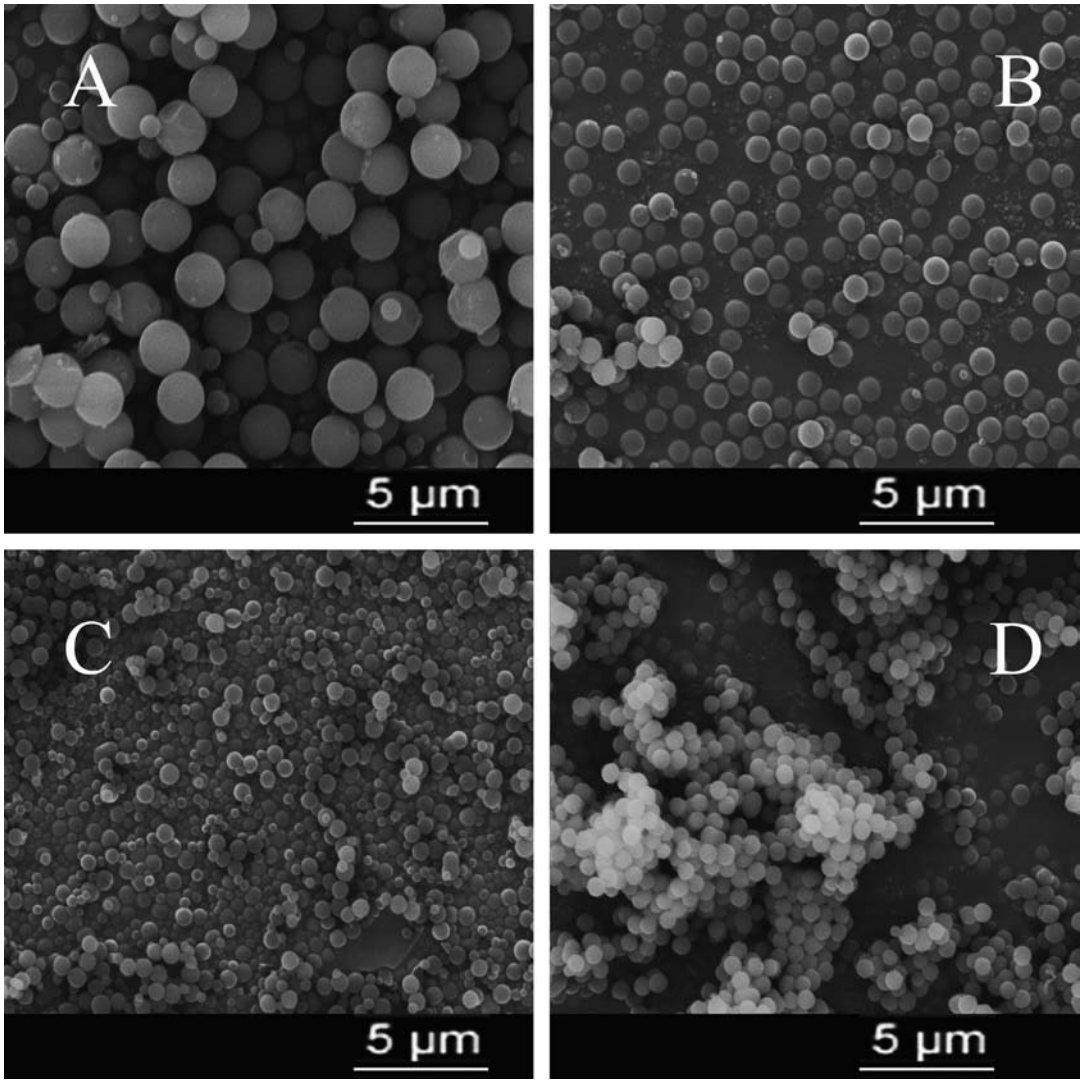

Fig. 1. SEM images of VFSS synthesized under different reactant ratio (A) TEOS: TVES=1.00: 4.55 (w/w); (B) TEOS: TVES=2.00: 4.55 (w/w); (C) TEOS: TVES=3.00: 4.55 (w/w); and (D) TEOS: TVES=4.00: 4.55 (w/w).

2.2. Synthesis of VFSS

Briefly, 13.65 g of VTES and 1.00 g of TEOS were dissolved in 150 mL of H_2O under strong magnetic stirring. A transparent solution was obtained after 3 h of stirring. 0.30 mL of $NH_3 \cdot H_2O$ was then added dropwise (60 s/ drop) to the solution using a 100 μL-Agilent Syringe. The reaction performed at 45 °C for 1 h. All of the products produced after the reaction were washed with H_2O and centrifuged (at 5000 rpm, for 10 min) for three times to remove the impurities. The resulting powders were then vacuum dried at 60 °C for 12 h. The reactant ratio, reaction time, temperature, and dripping speed of the $NH_3 \cdot H_2O$ were investigated to determine the effects of reaction conditions on the synthesis of the VFSS. Table S1 shows the conditions used during synthesis.

2.3. Modification of VFSS

The VFSS was modified as follows: 4.00 g of VFSS, 3.00 g of 1-octadecanethiol and 100 mg of AIBN were dissolved in 70 mL of toluene in a nitrogen atmosphere. The reaction was performed at 80 °C for 8 h. Afterwards, the products were successively washed with toluene, water and ethanol and vacuum dried at 60 °C for 12 h.

2.4. Characterization

Scanning electron microscopy (SEM) was performed using a FEI Quanta200. All of the samples were sprayed with gold (thickness about 10 nm) before analysis was performed. The sizes of the spheres were obtained by measuring the diameters of 100

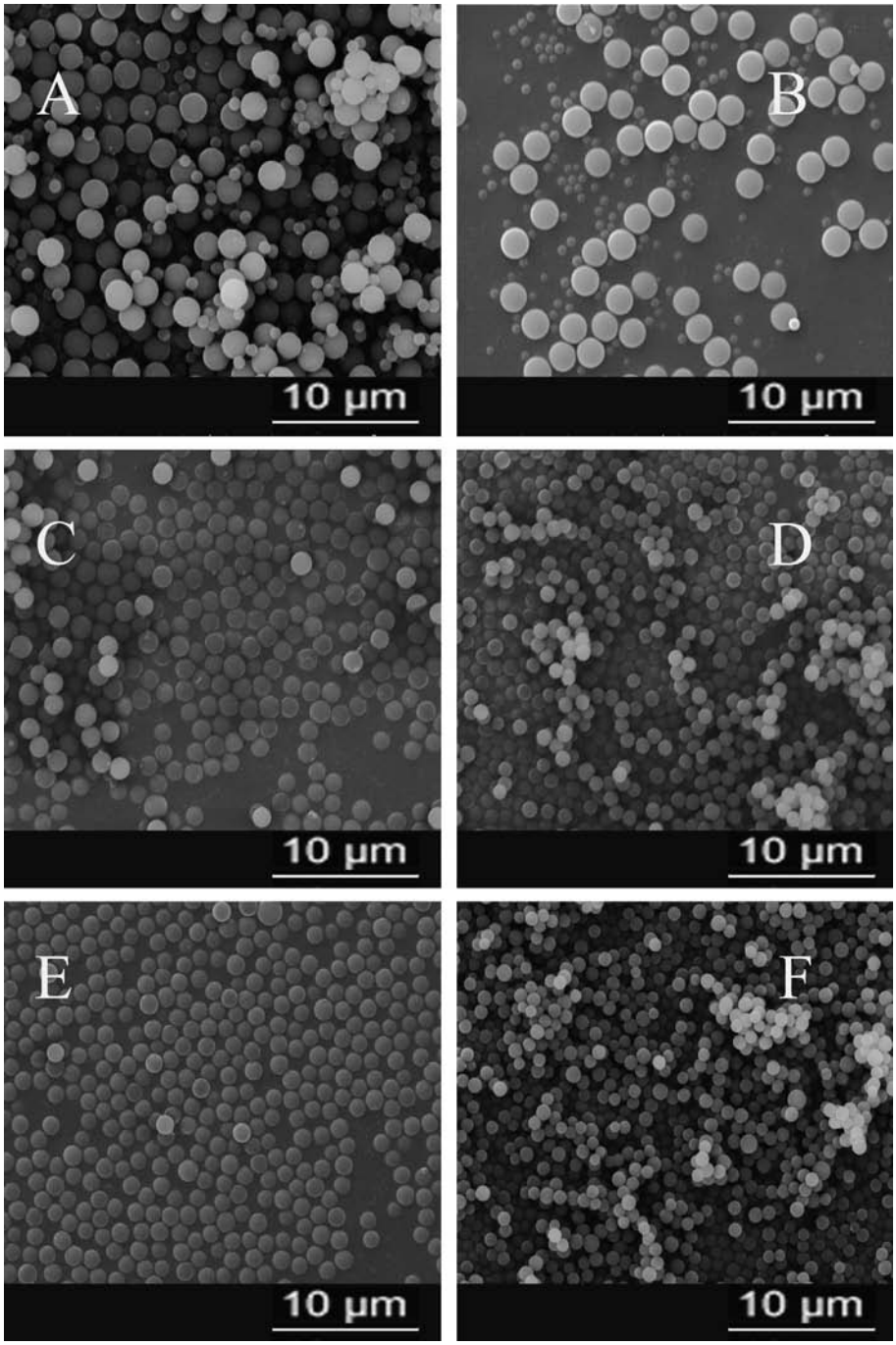

Fig. 2. SEM images of VFSS synthesized under different temperature (A) 25 °C; (B) 35 °C; (C) 45 °C; (D) 55 °C; (E) 65 °C; and (F) 75 °C.

spheres in the SEM image and calculating the mean diameter. Fourier transform infrared spectroscopy analysis (FT-IR) of the silica spheres was performed using Vertex 70. The contents of carbon and hydrogen in the samples were quantified using a Euro EA elemental analyzer. The pore volume was measured by a Quantachrome Nova 1000e surface area and pore size analyzer using the adsorption data through the BJH method. The contact angles of the VFSS and C-VFSS were obtained using Dataphysics OCA 20.

Table 1
Mean diameter of big spheres synthesized under different temperature.

Sample	Temperature (°C)	Mean diameter (μm)	Relative standard deviation (RSD) (%)
1	25	1.92	3.0
2	35	1.87	4.7
3	45	1.36	4.5
4	55	1.00	5.1
5	65	1.19	5.4
6	75	0.93	7.6

2.5. Chromatographic application of VFSS and C-VFSS

The VFSS and C-VFSS were slurry-packed into stainless steel tubes (50 mm × 2.1 mm i.d.) using chloroform as the homogenate solvent at 45 MPa. Water and methanol (50/50, v/v) were used as the propulsion solvents.

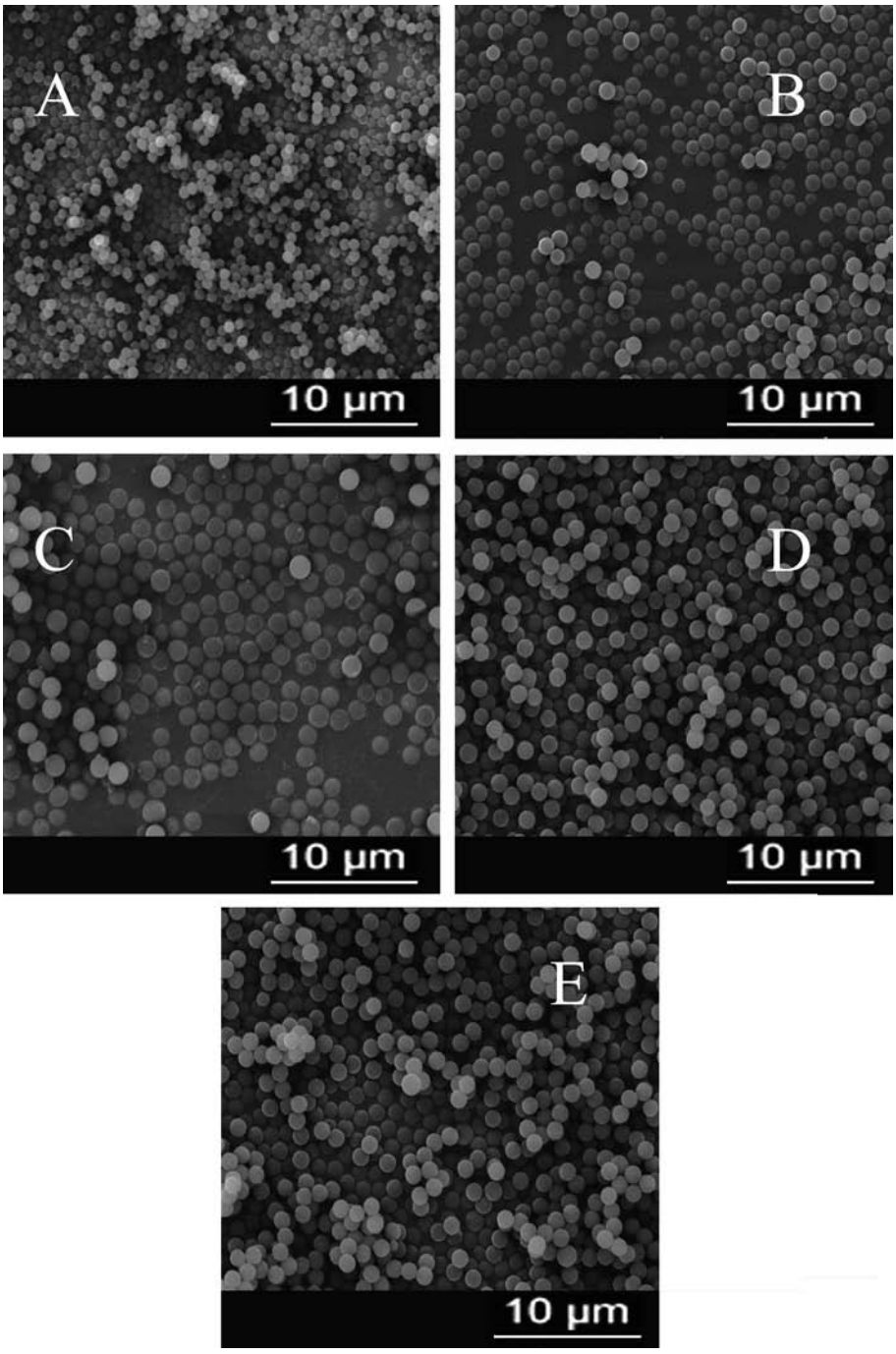

Fig. 3. SEM images of VFSS synthesized under different $NH_3 \cdot H_2O$ dripping speed (A) 10 s/drop; (B) 30 s/drop; (C) 60 s/drop; (D) 90 s/drop; and (E) 120 s/drop.

All chromatography experiments were performed on a HITACHI Elite Lachrom Ultra System equipped with L-2160U pump, L-2200 u autosampler, L-2400 u UV–vis detector and L-2300 column oven.

3. Results and discussion

3.1. Effects of reaction conditions on morphology and size of VFSS

Direct condensation of VTES is the easiest method to synthesize VFSS. Previous studies showed that reaction condition could effectively modify the morphology and particle size of VFSS [26–28]. However, in the present study, the yield of directly synthesized VFSS decreased sharply when the ratio of the VTES and $NH_3 \cdot H_2O$ increased and the dripping speed of $NH_3 \cdot H_2O$ reduced. Therefore, the TEOS is introduced to the system to increase the yield. A new organic-inorganic system is established when the TEOS is added to the system, and the effects of the main reaction factors under the new system are investigated.

Table 2
Mean diameter of VFSS synthesized under different $NH_3 \cdot H_2O$ dripping speed.

Sample	$NH_3 \cdot H_2O$ dripping speed (s/drop)	Mean diameter (μm)	RSD (%)
1	10	0.66	5.6
2	30	0.99	8.4
3	60	1.36	4.5
4	90	1.25	2.3
5	120	1.27	3.8

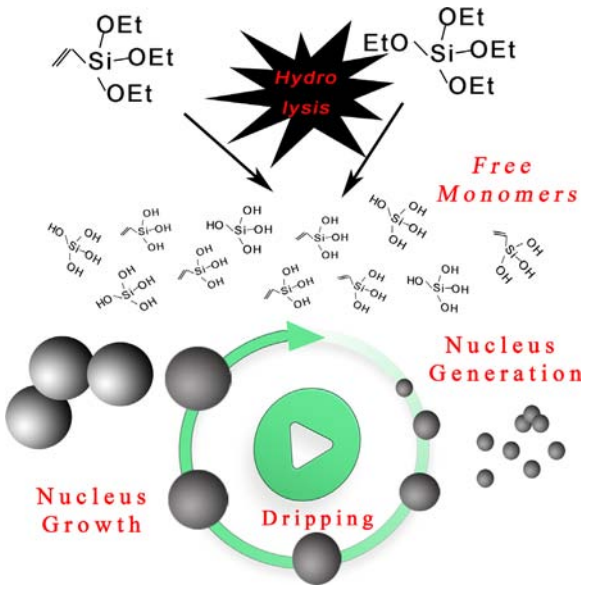

Fig. 4. Schematic illustration of the formation of VFSS.

3.1.1. Effect of TEOS amount

The TEOS is added to the system to accelerate the speed of condensation. Adding the TEOS greatly affected the system. Without the TEOS, the solution would remain transparent for hours after adding the $NH_3 \cdot H_2O$. On the contrary, the solution would turn turbid a few seconds after adding the $NH_3 \cdot H_2O$ when TEOS is present in the solution.

Moreover, the amount of TEOS significantly affected the morphology and particle size of the VFSS. The weight ratio of the TEOS and VTES changed from 1.00: 4.55 to 4.00: 4.55 in the study. Fig. 1 shows the SEM images of the samples produced. Large and small spheres formed when the concentration of the TEOS is low (TEOS: VTES = 1.00: 4.55). The diameters of the large spheres ranged from 1.87 μm to 2.09 μm, while the diameters of the small spheres ranged from 0.71 μm to 0.79 μm. The particle size of the large spheres kept decreased until all of them disappeared when the amount of the TEOS increased. Meanwhile, increasing the TEOS also increased the tendency of the particles to aggregate. The spheres are difficult to separate from each other when the ratio of the TEOS and VTES is 4.00: 4.55. Thus, we can conclude that increased amounts of TEOS could induce to smaller spheres and aggregation phenomenon. A tentative explanation on the effect of TEOS over the size of silica sphere will be provided in a subsequent paragraph.

3.1.2. Effect of temperature

Temperature is another important parameter that affects the particle size of the VFSS. In this experiment, temperature is also the key factor that eliminated small spheres in the product. When the reaction temperature increased from 25 °C to 75 °C, different results are obtained. Fig. 2 shows the SEM images of the samples produced. The number of small spheres decreased when the temperature increased. When reaction temperature achieved 45 °C, there were nearly no small spheres in the product. The variation trend in terms of particle size is complicated. Table 1 list the relationship between the temperature and particle size of the large spheres. The particle size decreased with increased temperature, except the particles produced between 55 °C and 65 °C. The mean diameter of 0.93 μm, which is the minimum diameter, is obtained when the temperature is 75 °C. A unique particle size rebound observed when the temperature increased from 55 °C to 65 °C. A similar phenomenon has been reported during direct condensation of VTES [27]. As the particle size of direct synthesized sphere decreased with the rising

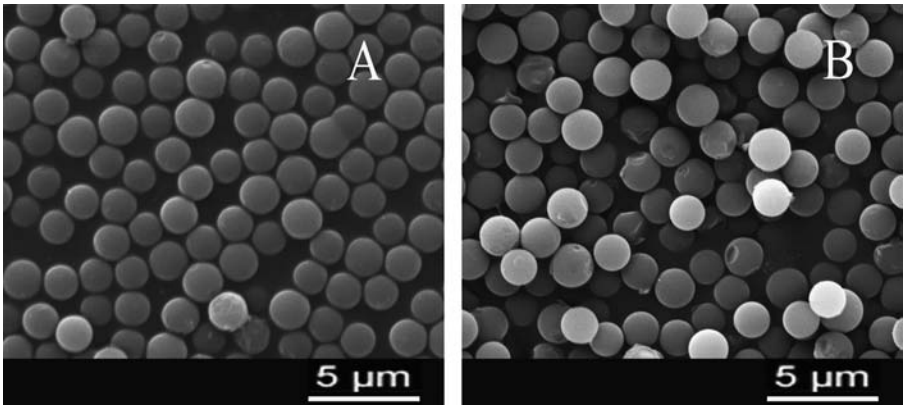

Fig. 5. SEM images of (A) VFSS and (B) C-VFSS.

of temperature at first, then went up when temperature exceeded a critical point. A tentative explanation on the effect of temperature will be provided in a subsequent paragraph. The temperature of 45 °C is chosen as the reaction temperature in succeeding experiments because this temperature is expected to produce uniform and large spheres.

3.1.3. Effect of $NH_3 \cdot H_2O$ dripping speed

This method utilized an extremely slow dripping speed of $NH_3 \cdot H_2O$, which is the main innovation in the method. A series of $NH_3 \cdot H_2O$ dripping speeds (10, 30, 60, 90, and 120 s/drop) are used to investigate the effect of the $NH_3 \cdot H_2O$ dripping speed. The enlarging effect of slow dripping speed is apparent for particle size. Fig. 3 shows the SEM images of the samples obtained using different dripping speed and Table 2 lists the measured diameters of the particles produced. When the dripping speed is 10 s/drop at first, the mean diameter of the particles is 0.66 μm. Decreasing the dripping speed leads to large particles. The largest mean diameter, which is 1.36 μm, is obtained when the dripping speed is 60 s/drop. However, the enlarging effect of low speed is limited. When the dripping speed is 90 s/drop, the mean diameter stopped increasing. Therefore, the dripping speed of $NH_3 \cdot H_2O$ was selected as 60 s/drop in the experiment. A tentative explanation on the effect of $NH_3 \cdot H_2O$ over the size of silica sphere will be provided in a subsequent paragraph.

3.1.4. Effect of reaction time

The effect of reaction time is also investigated by changing the reaction time from 1 h to 7 h. Fig. S1 shows the SEM images of the particles obtained when the reaction time is modified. No distinct difference in the morphology and particle size of the samples is observed. This finding means that the reaction occurred rapidly and extending the reaction time has no obvious influence on the morphology and size of the VFSS. Therefore, the reaction time was selected as 1 h in the experiment.

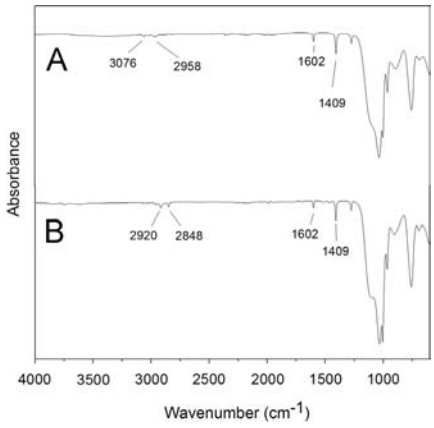

Fig. 6. FT-IR Spectra of (A) VFSS and (B) C-VFSS.

3.1.5. Explanation for the effect of reaction condition

Previous studies used a three-step model to describe the condensation of silica spheres [27,28,32]. In their model, the synthesis is subjected to three basic processes, including hydrolysis, nucleus generation, and nucleus growth. The model could successfully explain the direct VFSS synthesis procedure. However, it needs some revision to explain the formation of spheres with different sizes through the proposed method. The three-step model assumes that nucleus generation is far faster than nucleus growth, so it only happened at the start of the reaction and all the spheres grew simultaneously, leading to a uniform particle size of the products. But in the present system, the spheres are different in size, which can lead to the conclusion that the nucleus growth procedures for the spheres produced in the method are different.

Fig. 4 shows the revised model of condensation. As can be seen, the condensation procedure also consists of hydrolysis, nucleus generation and nucleus growth. However, we hypothesize that nucleus generation and nucleus growth form a number of different cycles during the reaction because slow dripping speed and low amount of $NH_3 \cdot H_2O$ enable the cycle to finish before the next drop of $NH_3 \cdot H_2O$ is introduced to the system. The revised model could be used to explain the phenomena in the experiments.

As mentioned above, TEOS effectively accelerates the condensation. The TEOS formed a lot of nuclei in the former cycles, which results in small spheres. However, the amount of TEOS decreases sharply in the latter cycles, therefore, nuclei are less and the size of spheres becomes larger. When the amount of TEOS increases, sufficient TEOS are provided in latter cycles, thus leading to the extinction of large spheres. Moreover, the aggregation tendency should be owing to a higher sphere concentration because of the increment of nuclei.

Temperature could influence the rate of hydrolysis, nucleus generation and nucleus growth simultaneously. More VTES could participate in the nucleus generation process when the temperature increases, thus the nuclei are formed with more VTES and less TEOS. When the temperature reaches 45 °C, the ratio of VTES and TEOS in nucleus meets the threshold to assure TEOS is adequate in the latter cycles, so the spheres become uniform. Furthermore, temperature increase accelerates the overall nucleus generation rate, leading to the decline of diameter of spheres. However, a size rebound between 55 °C and 65 °C is observed, which indicates that the increment of hydrolysis is larger than that of nucleus generation during the temperature interval.

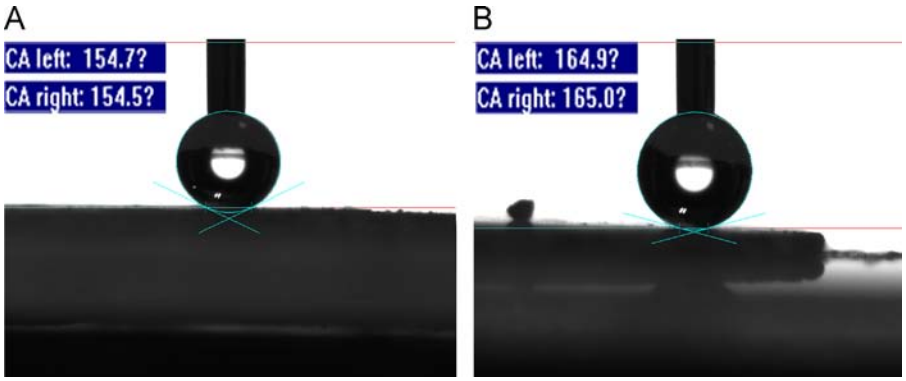

Fig. 7. Contact angle of (A) VFSS and (B) C-VFSS.

The results obtained using different $NH_3 \cdot H_2O$ dripping speeds are also consistent with the cycle-model. Slow $NH_3 \cdot H_2O$ dripping speed extends the time for nucleus growth in every cycle, thus the spheres enlarge. Nevertheless, the enlarging effect of extending time interval is confined by thermodynamics. When the diameter of spheres reaches its thermodynamic maximum, the nucleus growth stops and the cycle is completed. It can be confirmed from the data that 60 s are enough for the cycles to complete. The result from different reaction times also shows that the time for cycles to complete is short.

3.2. Characterization of VFSS and C-VFSS

By using the method written in 2.2, the diameter of the VFSS increased to 1.82 μm, which is suitable for HPLC packing material. Moreover, the VFSS were modified by C_{18} groups through the "thiol-ene" click reaction. Fig. 5 shows the SEM images of the VFSS and C-VFSS produced. As the pictures illustrate, the spheres before modification are well-spherical and uniform. Even though some small defects are observed on the surface of C-VFSS after the "thiol-ene" modifying, the morphology of the material remains uniform spheres.

FT-IR and elemental analysis are used to confirm the functional groups present in the materials. Fig. 6 shows the FT-IR spectra of VFSS and C-VFSS. According to previous studies [2,33,34], the peak at 757 cm^{-1} corresponds to a Si–C stretching vibration band, and a peak at 1043 cm^{-1} derives from Si–O–Si stretching vibration. A peak at 996 cm^{-1} is due to a C=C vibration of terminal olefin. Peaks at 1602 cm^{-1} and 1409 cm^{-1} are associated with C=C and C–H vibrations of vinyl groups. Peaks at 3076 $cm^{-1}$and 2958 cm^{-1} correspond to asymmetrical and symmetrical stretching vibrations of $=CH_2$. FT-IR results illustrate that vinyl groups are successfully introduced into VFSS. The spectrum of the C-VFSS shows another two peaks at 2920 cm^{-1} and 2848 cm^{-1} compared with that of the VFSS. These peaks correspond to the stretching of $-CH_3$ and $-CH_2$ in C_{18} groups. Meanwhile, the peaks at 1602 cm^{-1} and 1409 cm^{-1} in the C-VFSS spectra indicate that there are still a lot of vinyl groups in C-VFSS.

The elemental analysis shows that the total contents of carbon and hydrogen are 20.17%, and 3.94% for VFSS, as well as 22.43%,

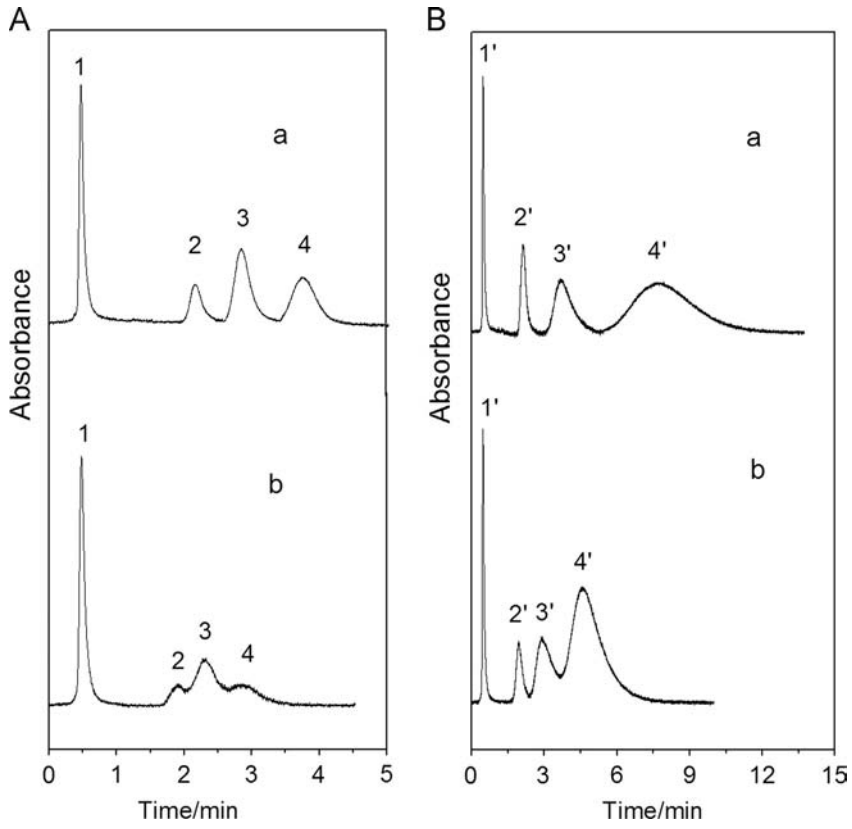

Fig. 8. Separation of (A) benzene homologs and (B) non-polar compounds with different ring content on (a) C-VFSS column and (b) VFSS column. Conditions: (A) mobile phase: water/acetonitrile mixture (50/50; v/v); flow rate: 0.2 mL/min; UV detection at 254 nm; (B) mobile phase: water/ acetonitrile mixture (50/50; v/v); flow rate: 0.2 mL/min; UV detection at 254 nm. Peak identity: (A) 1, uracil; 2, benzene; 3, toluene; 4, meta-xylene; (B) 1', uracil; 2', benzene; 3', phenanthrene; 4', fluoranthene.

Table 3
Retention time and retention Factor of VFSS and C-VFSS for benzene homologs under the same separation condition.

Solutes	Rentention time (VFSS Column) (min)	k' (VFSS Column)	Rentention time (C-VFSS Column)/min	k' (C-VFSS Column)
Uracil	0.46	/	0.46	/
Benzene	1.90	3.13	2.12	3.61
Toluene	2.30	4.00	2.80	5.09
Meta-xylene	2.88	5.26	3.66	6.96

and 4.10% for C-VFSS, respectively. The Carbon content of VFSS illustrates that the vinyl groups are abundant in VFSS, and the carbon content growth in C-VFSS proves that the particles are successfully modified by the C_{18} groups.

Pore characteristic is another important characteristic of a packing material. The Brunauer–Emmett–Teller method is used to measure the pore volume of VFSS and C-VFSS. The pore volumes of the VFSS and C-VFSS are 0.013 $cm^3 g^{-1}$ and 0.012 $cm^3 g^{-1}$ respectively, which means that the materials exhibit a non-porous structure. According to the literatures, non-porous spheres are beneficial for fast separation, however, loading capacity of non-porous spheres is low [30,31].

Except the high chemical activity, vinyl groups also show strong hydrophobicity because of their unique structure [33,35]. Furthermore, the introduction of C_{18} could provide a higher hydrophobicity to C-VFSS. Contact angles are determined by a contact angle goniometer to examine the hydrophobicity of VFSS and C-VFSS, and the results are shown in Fig. 7. The contact angle of VFSS and C-VFSS reached 154.7° and 165.0°, respectively. Thus, the VFSS and C-VFSS synthesized by the method exhibit super-hydrophobicity, which indicates that the materials could be used to separate nonpolar substances.

3.3. Chromatographic performance of VFSS and C-VFSS

Three homologs of benzene (i.e.,benzene, toluene, and meta-xylene) were selected to test the chromatographic performance of the VFSS and C-VFSS columns. In the experiments, uracil was used to measure the void volume of the column. Fig. 8A shows the chromatograms obtained when the homologs of benzene are separated using the fabricated columns. The pressures of VFSS column and C-VFSS column under the operating condition are 17.1 MPa and 16.9 MPa, respectively. The high pressure is mainly owing to the small particle size and the non-porous structure. Table 3 lists the retention times and retention factors (k') of the compounds analyzed. The C-VFSS column could effectively separated the three homologs within 4 min. However, the peaks of the three homologs overlapped partly on the chromatogram of the VFSS column under the same separation condition. The eluting order of the VFSS and C-VFSS columns are in accordance with the hydrophobicity of the three solutes, which means that the VFSS and C-VFSS exhibit hydrophobic retention behavior. VFSS is less hydrophobic than C-VFSS, therefore, the retention factors of the VFSS column are lower than that of the C-VFSS column.

A series of nonpolar compounds with different ring contents (i.e.,benzene, phenanthrene, and fluoranthene) were chosen to further prove the hydrophobic retention behaviors of the VFSS and C-VFSS columns. Fig. 8B shows the chromatograms obtained when the nonpolar compounds with different ring contents are subjected to chromatographic analysis. Both the VFSS and C-VFSS columns separated the three kinds of nonpolar compounds. The eluting order of the columns are consistent with the hydrophobicity order of the three solutes, and the retention time on the C-VFSS column is longer than that on the VFSS column. The separation performance implies that the retention behavior is mainly decided by the hydrophobicity of solutes.

Despite of hydrophobicity, the unsaturated structure of vinyl groups may provide some different kinds of retention behaviors to the packing material. Previous articles have mentioned that the π–π electro–donor–acceptor (EDA) mechanism may participate in the chromatographic retention behavior of conjugated system [36–38]. π–π EDA is a specific force existing between electron–donor and electron–acceptor moieties, which involves one electron transfer from the highest occupied molecular orbital of donor to the lowest unoccupied molecular orbital of acceptor and forms a weak covalent bond by the unpaired electrons [36]. Both the VFSS and C-VFSS contained abundant vinyl groups on the surface, thus, the materials have the potential for exhibiting π–π EDA retention mechanism. A series of aniline derivatives (i.e., aniline, p-chloroaniline, and p-nitroaniline) were selected to testify the participation of π–π EDA retention mechanism. The experiments were performed on the VFSS column because its hydrophobic retention behavior is weaker than that of the C-VFSS column, which means that π–π EDA effect would be more obvious. The chromatograms are shown in Fig. 9, and

Table 4
Retention Time of aniline derivatives on VFSS Column under different mobile phase.

Solutes	Retention time (80% water 20% acetonitrile, v/v) (min)	Retention time (40% water 60% acetonitrile, v/v) (min)
aniline	2.21	0.80
p-nitroaniline	2.28	0.62
p-chloroaniline	5.66	0.88

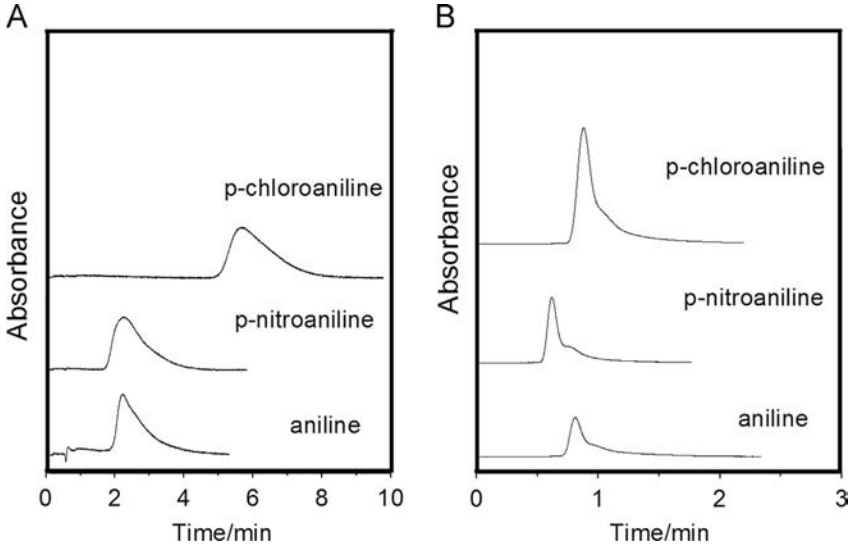

Fig. 9. Chromatograms of aniline, p-nitroaniline and p-chloroaniline on VFSS using different mobile phase. (A) mobile phase: water/acetonitrile mixture (80/20, v/v); flow rate: 0.2 mL/min; UV detection at 254 nm; (B) mobile phase: water/acetonitrile mixture (40/60, v/v); flow rate: 0.2 mL/min; UV detection at 254 nm.

Table 5
Reproducibility of VFSS column and C-VFSS column (n= 5)[a].

	Benzene		Phenanthrene		Fluoranthene	
	RSD of retention time (%)	RSD of peak areas (%)	RSD of retention time (%)	RSD of peak areas (%)	RSD of retention time (%)	RSD of peak areas (%)
Run-to-run (VFSS column)	0.33	1.3	0.24	1.1	0.15	1.3
Day-to-day (VFSS column)	0.99	2.9	0.91	2.1	0.85	2.2
Run-to-run (C-VFSS column)	0.15	1.5	0.28	1.2	0.15	0.95
Day-to-day (C-VFSS column)	1.2	2.3	0.87	2.1	0.60	2.7

[a] Experimental conditions were identical to Fig. 8B.

the retention times are listed in Table 4. Aniline eluted first, followed by p-nitroaniline, and p-chloroaniline. This eluting order is observed when the mobile phase consists of 80% water and 20% acetonitrile (v/v). This result is in accordance with the hydrophobicity sequence of the solutes. When the mobile phase is composed of 40% water and 60% acetonitrile (v/v), the effect of the hydrophobic retention behavior decreased and the eluting order changed into p-nitroaniline, aniline, and p-chloroaniline. The new eluting order is different from the hydrophobicity sequence; however, it is consistent with the electron donating ability sequence of the compounds. p-Nitroaniline exhibits the weakest electron donating ability because of the electron-withdrawing effect of nitro group. p-Chloroaniline behaves as the strongest electron-donor because of its lone pair of electrons of chlorine. The eluting order may be explained by the π–π EDA mechanism. The vinyl groups on the material are electron-deficient, thus, it can build a stronger π–π EDA interaction with stronger electron–donors.

From the data above, a conclusion could be reached that π–π EDA mechanism participated in the retention behavior of vinyl groups. However, the effect of the π–π EDA mechanism only can be observed when the hydrophobic retention behavior is restrained.

3.4. Reproducibility

The reproducibility of VFSS column and C-VFSS column were investigated in terms of the separating performance of benzene, phenanthrene, and fluoranthene. The RSDs of retention time and peak areas are listed in Table 5. As can be seen from the table, the run-to-run RSDs ($n=5$) of retention time and peak areas on both VFSS column and C-VFSS column are less than 0.33% and 1.5%, respectively. The day-to-day RSDs ($n=5$) of retention time and peak areas are less than 1.2% and 2.9%. Moreover, both columns were used for at least 200 times of operations over the course of 1 month without observable changes in the separation performance. The results indicate that both VFSS-column and C-VFSS column have good reproducibility and stability.

4. Conclusion

The effects of the amount of TEOS, temperature, $NH_3 \cdot H_2O$ dripping speed, and reaction time on the morphology and particle size of the VFSS are investigated in this research. The result shows that low TEOS concentration, slow $NH_3 \cdot H_2O$ dripping speed and 45 °C is beneficial for the formation of uniform large spheres. A cycle-model is put forward to explain the effects of reaction conditions. By changing the reaction conditions, uniform sub-2 μm VFSS are obtained through one-step method. Moreover, the VFSS could be successfully modified by C_{18} groups through a "thiol-ene" click reaction. Both VFSS and C-VFSS exhibit strong hydrophobicity and could be used as stationary phase to effectively separate nonpolar compounds. Besides hydrophobic retention behavior, vinyl groups can also provide a π–π EDA retention mechanism during separation.

Acknowledgments

This project was supported by the National Natural Science Foundation of China (No. 21075074).

Appendix A. Supporting information

Supplementary data associated with this article can be found in the online version at http://dx.doi.org/10.1016/j.talanta.2014.11.044.

References

[1] T. Watanabe, K. Makitsuru, H. Nakazawa, S. Hara, T. Suehiro, A. Yamamoto, T. Hiraide, T. Ogawa, Anal. Chim. Acta 386 (1999) 69–75.
[2] S. Chen, X. Zhang, Q. Han, M.Y. Ding, Talanta 101 (2012) 396–404.
[3] Y. Ma, L. Qi, J. Ma, Y. Wu, O. Liu, H. Cheng, Colloids Surf., A 229 (2003) 1–8.
[4] C.-X. Yang, X.-P. Yan, Anal. Chem. 83 (2011) 7144–7150.
[5] W. Stöber, A. Fink, E. Bohn, J. Colloid Interface Sci. 26 (1968) 62–69.
[6] H. Kanazawa, K. Yamamoto, Y. Matsushima, N. Takai, A. Kikuchi, Y. Sakurai, T. Okano, Anal. Chem. 68 (1996) 100–105.
[7] Y. Wang, T.-T. Ong, L.-S. Li, T.T.Y. Tan, S.-C. Ng, J. Chromatogr. A 1216 (2009) 2388–2393.
[8] Z. Guo, A. Lei, X. Liang, Q. Xu, Chem. Commun. (2006) 4512–4514.
[9] H.C. Kolb, M. Finn, K.B. Sharpless, Angew. Chem. Int. Ed. 40 (2001) 2004–2021.
[10] T. Posner, Ber. Dtsch. Chem. Ges 38 (1905) 646–657.
[11] K.L. Killops, L.M. Campos, C.J. Hawker, J. Am. Chem. Soc. 130 (2008) 5062–5064.
[12] V.T. Huynh, G. Chen, P.d. Souza, M.H. Stenzel, Biomacromolecules 12 (2011) 1738–1751.
[13] N. Ten Brummelhuis, C. Diehl, H. Schlaad, Macromolecules 41 (2008) 9946–9947.
[14] L.M. Campos, I. Meinel, R.G. Guino, M. Schierhorn, N. Gupta, G.D. Stucky, C.J. Hawker, Adv. Mater. 20 (2008) 3728–3733.
[15] A. Shen, Z. Guo, L. Yu, L. Cao, X. Liang, Chem. Commun. 47 (2011) 4550–4552.
[16] A. Shen, Z. Guo, X. Cai, X. Xue, X. Liang, J. Chromatogr. A 1228 (2012) 175–182.
[17] A. Shen, X. Li, X. Dong, J. Wei, Z. Guo, X. Liang, J. Chromatogr. A 1314 (2013) 63–69.
[18] K. Wang, Y. Chen, H. Yang, Y. Li, L. Nie, S. Yao, Talanta 91 (2012) 52–59.
[19] X.T. Peng, T. Liu, S.X. Ji, Y.Q. Feng, J. Sep. Sci. 36 (2013) 2571–2577.
[20] M.-L. Chen, J. Zhang, Z. Zhang, B.-F. Yuan, Q.-W. Yu, Y.-Q. Feng, J. Chromatogr. A 1284 (2013) 118–125.
[21] Y. Chen, K. Wang, H. Yang, Y. Liu, S. Yao, B. Chen, L. Nie, G. Xu, J. Chromatogr. A 1233 (2012) 91–99.
[22] Z. Zhang, M. Zhang, Y. Liu, X. Yang, L. Luo, S. Yao, Sep. Purif. Technol. 87 (2012) 142–148.
[23] P.T. Vallano, V.T. Remcho, J. Chromatogr. A 887 (2000) 125–135.
[24] H. Pu, X. Zhang, J. Yuan, Z. Yang, J. Colloid Interface Sci. 331 (2009) 389–393.
[25] Y. Takeda, Y. Komori, H. Yoshitake, Colloids Surf. A 422 (2013) 68–74.
[26] T.-S. Deng, Q.-F. Zhang, J.-Y. Zhang, X. Shen, K.-T. Zhu, J.-L. Wu, J. Colloid Interface Sci. 329 (2009) 292–299.
[27] J. Yin, T. Deng, G. Zhang, Appl. Surf. Sci. 258 (2012) 1910–1914.
[28] T.-S. Deng, J.-Y. Zhang, K.-T. Zhu, Q.-F. Zhang, J.-L. Wu, Colloids Surf., A 356 (2010) 104–111.
[29] J.S. Mellors, J.W. Jorgenson, Anal. Chem. 76 (2004) 5441–5450.
[30] J.E. MacNair, K.C. Lewis, J.W. Jorgenson, Anal. Chem. 69 (1997) 983–989.

[31] L. Tolley, J.W. Jorgenson, M.A. Moseley, Anal. Chem. 73 (2001) 2985–2991.
[32] V.K. LaMer, R.H. Dinegar, J. Am. Chem. Soc. 72 (1950) 4847–4854.
[33] Q. Shang, M. Wang, H. Liu, L. Gao, G. Xiao, J. Coat. Technol. Res. 10 (2013) 465–473.
[34] H. Zhou, Y. Xu, H. Tong, Y. Liu, F. Han, X. Yan, S. Liu, J. Appl. Polym. Sci. 128 (2013) 3846–3852.
[35] L. Xue, J. Li, J. Fu, Y. Han, Colloids Surf., A 338 (2009) 15–19.
[36] X. Zhang, S. Chen, Q. Han, M. Ding, J. Chromatogr. A 1307 (2013) 135–143.
[37] S. Zhang, Z. Du, G. Li, Anal. Chem. 83 (2011) 7531–7541.
[38] D. Zhu, J.J. Pignatello, Environ. Sci. Technol. 39 (2005) 2033–2041.